Orientation of Thiophenol Adsorbed on Silver Determined by Nonlinear Vibrational Spectroscopy of the Carbon Skeleton

A. A. Mani,[†] Z. D. Schultz,[‡] Y. Caudano,*[,†] B. Champagne,[§] C. Humbert,[†] L. Dreesen,[†] A. A. Gewirth,[‡] J. O. White,[‡] P. A. Thiry,[†] and A. Peremans[†]

Laboratoire de Spectroscopie Moléculaire de Surface, Facultés Universitaires Notre-Dame de la Paix, Rue de Bruxelles, 61, B-5000 Namur, Belgium, Frederick Seitz Materials Research Laboratory, University of Illinois at Urbana-Champaign, 104 S. Goodwin Avenue, Urbana, Illinois 61801, and Laboratoire de Chimie Théorique Appliquée, Facultés Universitaires Notre-Dame de la Paix, Rue de Bruxelles, 61, B-5000 Namur, Belgium

Received: December 1, 2003; In Final Form: July 28, 2004

The orientation of thiophenol adsorbed on silver is determined by comparing ab initio calculated and experimental sum-frequency generation (SFG) spectra measured between 9 and 20 μm using a tandem KTP/CdSe optical parametric oscillator. The molecule S−C bond is tilted ∼37° from the surface normal with the aromatic ring plane perpendicular to the surface.

I. Introduction

Organic conjugated systems possess a high potential for use as active components in electronic, optoelectronic, and photonic devices. In addition to their high electrical conductivity exploited in such applications as antistatic coatings,[1,2] they present fast and large nonlinear optical responses[3] and can be used in field-effect transistors, light-emitting diodes, solid-state lasers, photovoltaic devices, biosensors,[1] and molecular electronics.[4] Organic compounds can operate as nanometer-scale electronic transistors, rectifiers, or conducting wires.[5] In most of these applications, anchoring the molecules to a metallic electrode plays a crucial role. Therefore, characterization and monitoring of the interfacial conformation of the system is of paramount importance.

Thiophenol (TP) is a model system extensively studied to evaluate the conductivity between metallic electrodes and the body of conjugated molecules.[6] The adsorption configuration of TP on gold single-crystal surfaces has been extensively studied using surface-enhanced Raman spectroscopy (SERS),[7] angular resolved ultraviolet photoemission spectroscopy (ARUPS),[8] high-resolution electron energy loss spectroscopy (HREELS),[8,9] infrared reflection absorption spectroscopy (IRAS),[10] ellipsometry,[11] and scanning tunneling spectroscopy.[12] Depending on the preparation conditions and surface coverage, TP layers are either disordered[10−12] or organized with the phenyl ring slightly tilted,[7] strongly tilted,[9] or quasi-parallel to the substrate surface.[8] Yet, the orientation of TP adsorbed on the other s-band metals, such as silver[13] and copper,[14] or on the d-band transition metals, such as Ni(111),[11] is much less documented.

In this work, we used sum-frequency generation (SFG) spectroscopy to determine the adsorption configuration of TP on Ag. To investigate the rise in complexity of the vibrational signature of larger conjugated molecules, we also recorded the SFG spectrum of 2-naphthalenethiol (NTT) self-assembled monolayers (SAM) on Ag. The strict selection rules of SFG spectroscopy lead to simple vibrational signatures with respect to linear spectroscopies such as SERS, HREELS, and IRAS. Furthermore, SFG is highly sensitive to film order, azimuthal anisotropy,[15] and admolecule conformation.[16,17] Unfortunately, the spectral range of standard SFG setups is limited by the tabletop laser source to the 2.5−9 μm interval. Therefore, the exploitation of the SFG advantages has been restricted mainly to the CH vibrations of the headgroups[15] of alkanethiol SAM. Hereafter, we demonstrate that SFG spectroscopy of the carbon skeleton in the mid-infrared between 9.5 and 20 μm enables one to determine the orientation of more complex conjugated systems relevant to molecular electronics, thanks to the strong, nonlinear dipolar activity associated to the carbon framework deformations.[3,18] For this study, we used a newly developed tabletop laser system providing a beam of several mW, continuously tunable from 9.5 to 20 μm (1050 to 500 cm^{-1}), with a resolution better than 2 cm^{-1}.

II. Experimental Section

The tunable infrared beam is generated by a Nd:YAG laser mode-locked with a nonlinear mirror[19,20] that pumps synchronously a picosecond KTP optical parametric oscillator (OPO) followed by a CdSe crystal performing difference-frequency generation (DFG) from the signal and idler beams produced in the KTP OPO.[21] The laser operates at 25 Hz and delivers about a hundred single pulses (duration ≈ 10 ps) per laser burst (duration ≈ 1 μs). The OPO is tunable between 475 and 1050 cm^{-1}, with a beam power of 2 mW at 670 cm^{-1} (corresponding to an energy of ∼0.8 μJ per pulse). The visible pulses at 532 nm are generated by frequency doubling a third of the YAG pump in a BBO crystal. The visible power is 8 mW (∼0.8 μJ per pulse).

The *p*-polarized infrared and visible laser beams impinge onto the sample with incidence angles of 65° and 55°, respectively. To remove the 532 nm light, the *p*-polarized SFG beam passes through a spatial filter and a holographic notch filter. The beam

* Corresponding author.
[†] Laboratoire de Spectroscopie Moléculaire de Surface, Facultés Universitaires Notre-Dame de la Paix.
[‡] University of Illinois at Urbana-Champaign.
[§] Laboratoire de Chimie Théorique Appliquée, Facultés Universitaires Notre-Dame de la Paix.

10.1021/jp037661d CCC: $27.50
Published on Web 09/21/2004

is then dispersed in a double monochromator and detected by a photomultiplier.

III. Results and Discussion

Predominantly (111) Ag substrates are prepared by evaporation onto mica. The SAMs are obtained after 24 h immersion of the substrates in ethanol solutions containing 1.0 mM of TP or NTT. The SFG spectrum of TP SAM, acquired by tuning the mid-IR OPO from 9.5 to 20 μm, has two dominant peaks located at $\sim$1000 cm^{-1} and $\sim$690 cm^{-1} (Figure 1), in accordance with those obtained previously with a free electron laser[22] and with an OPO at 10 μm.[23]

To extract the TP SAM conformation, the experimental data are compared with ab initio theoretical SFG spectra. Briefly, the ground-state geometry of the molecule was fully optimized using the 6-311++G(d,p) atomic basis set within the hybrid B3LYP[24] DFT scheme. This was achieved with the Gaussian98 program,[25] under the condition that the residual forces are less than 10^{-5} a.u. For these optimized geometries the harmonic vibrational frequencies ω_ν and normal modes Q_ν were determined analytically using the coupled-perturbed Kohn−Sham (KS) technique (see, e.g., ref 26) within the B3LYP/6-311++G-(d,p) scheme. To compensate for the lack of anharmonicity, the limits of the treatment of electron correlation,[27] and the absence of the Ag substrate, the frequencies were scaled by a factor of 0.97. The dynamic dipole vector $\partial\mu/\partial Q_\nu$ for each vibration Q_ν at the equilibrium geometry and the corresponding harmonic IR intensities were computed analytically from the first-order nuclear coordinate derivatives of the KS orbitals. The Raman tensors $\partial\alpha/\partial Q_\nu$ were evaluated using a numerical differentiation procedure where the static polarizability tensor was calculated for different structures resulting from the addition of different fractions of the normal coordinate to the equilibrium geometry.[28] The use of four distorted geometries per vibrational normal mode enabled an accuracy of 1% or better on the polarizability derivatives and the related harmonic Raman intensities.

The relevant vibrational modes in the range 500−1050 cm^{-1} are shown in Figure 2. The simulated SFG signatures are then calculated according to

$$I_{\mathrm{SFG}}(\omega_{\mathrm{IR}}) \propto \left| |\chi_{\mathrm{nr}}| e^{i\phi_{\mathrm{nr}}} + \sum_{\nu=1}^{n} \frac{\sum_{ijk} F_{ijk}^{ppp} \left\langle \sum_{lmn} T_{lmn\rightarrow ijk} \frac{\partial \alpha_{lm}}{\partial Q_\nu} \frac{\partial \mu_n}{\partial Q_\nu} \right\rangle}{\omega_\nu - \omega_{\mathrm{IR}} - i\Gamma_\nu} \right|^2 \quad (1)$$

This formula assumes a homogeneous orientation of the admolecule defined by the angles θ and ξ (Figure 1), and the existence of randomly oriented molecular domains on the crystal surface, accounting for the effective azimuthal isotropy of the adlayer and represented by the angle brackets. T is the transform matrix from the molecular axes to the laboratory frame, and F contains the Fresnel factors for *ppp* polarization.[29] Γ_ν is the homogeneous broadening of each Lorentzian vibration, and χ_{nr} is the substrate nonresonant contribution, with amplitude $|\chi_{\mathrm{nr}}|$ and phase ϕ_{nr}. To decrease the number of free parameters (the angles θ and ξ fixing the molecule orientation, the amplitude $|\chi_{\mathrm{nr}}|$ and phase ϕ_{nr} of the substrate nonresonant susceptibility, and the vibrational line widths Γ_ν), we compared the experimental and theoretical curves assuming $\Gamma_\nu = 6$ cm^{-1} for each vibration, in concordance with the experimental width of the resonances. Furthermore, in the theoretical simulations presented in Figure 3, for each couple of angles θ and ξ, we adjusted the substrate nonresonant contribution χ_{nr} to reproduce the experimentally observed ratio of the maximum SFG peak intensity to the nonresonant signal at long wavelengths, as well as the experimental line shape of the modes. The latter simplification does not affect much the interpretation if the observed substrate nonresonant contribution is weak with respect to the observed SFG resonances.

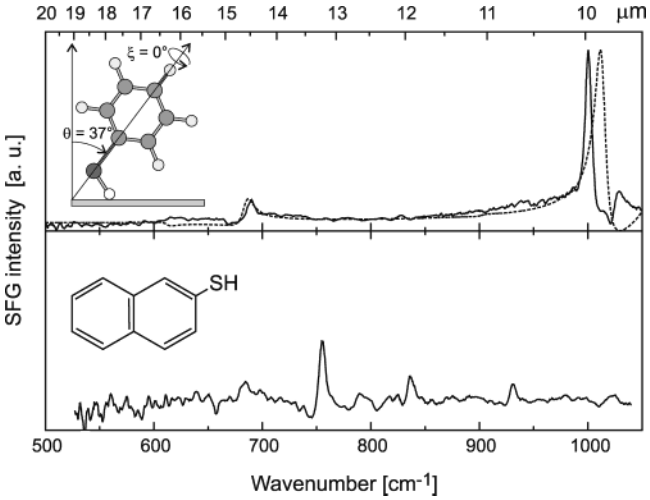

Figure 1. (Top) Experimental SFG spectrum of thiophenol/Ag(111) (continuous line) and best theoretical fit (dotted line). (Bottom) SFG spectrum of 2-naphthalenethiol/Ag(111).

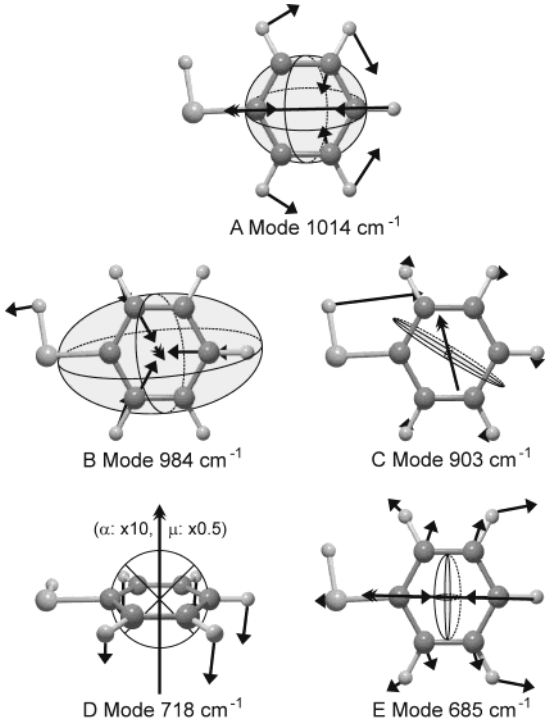

Figure 2. Ab initio vibrational modes of thiophenol along with schematic representations of the infrared dipoles (double arrows) and Raman tensors (ellipsoids).

According to the calculations, one intense SFG peak is present between 950 and 1050 cm^{-1} (A mode at 1014 cm^{-1}). The mode corresponds to an in-plane ring deformation that shows a dipole moment quasi-parallel to the S−C bond and a strong Raman activity, which is nearly isotropic in the ring plane (Figure 2). Predominant SFG features in the 650−750 cm^{-1} range arise from two modes, which exhibit totally different spectral properties. One vibration corresponds to an out-of-plane deformation of the ring CH bonds (D mode at 718 cm^{-1}). It has

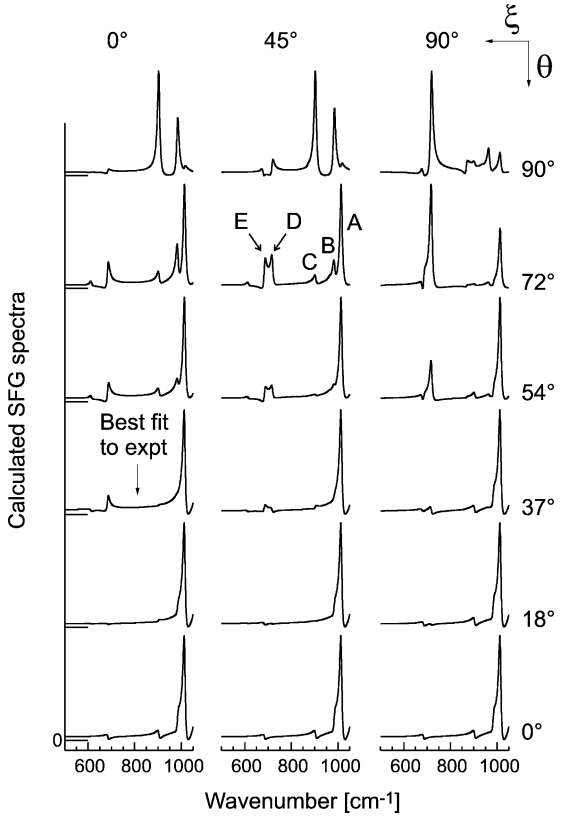

Figure 3. Ab initio theoretical SFG spectra of thiophenol/Ag for *ppp* polarization (with 65° and 55° incidence angles for IR and visible beams, respectively). Each spectrum was normalized to the intensity of its strongest peak.

much weaker Raman activity and an infrared dipole oriented perpendicular to the ring plane, in a direction where off-diagonal elements of the Raman tensor dominate. The second contribution arises from an in-plane ring deformation characterized by a strong infrared dipole quasi-aligned with the S−C bond (E mode at 685 cm^{-1}). The corresponding "dish-shaped" ellipsoid representing its Raman activity tensor exhibits significant amplitude in the plane perpendicular to the S−C bond. The comparison of the theoretical and experimental frequencies suggests that the SFG peaks at ∼690 cm^{-1} and ∼1000 cm^{-1} must be assigned to the E and A modes, respectively. The calculations also predict two other SFG-active modes, which are not observed: the B and C modes at 984 and 903 cm^{-1}, respectively. The B mode corresponds to an in-plane vibration of the TP ring. It has a strong Raman activity but a weak, in-plane, IR dipole that result in a weak SFG intensity for most molecule orientations. The C mode involves mainly the bending vibration of the SH bond (Figure 2) and, thus, should not be observed in the case of adsorbed TP.

The comparison of the relative intensities of all these distinct features will enable the unambiguous determination of the TP orientation. Indeed, the screening of the metal surface entails the dominance of the F_{zzz}^{ppp} term in eq 1. The A and E modes exhibit dipole moments parallel to the S−C axis and a similar shape of their Raman tensors around this axis. Since, on the other hand, they present contrasting Raman activity along the S−C axis, their relative SFG intensity is thus mainly determined by the angle θ. The intensity of the A mode is maximum for the S−C axis normal to the metal surface, i.e., $\theta = 0°$. For the E mode, the infrared dipole and Raman tensor act as cross polarizer for the three IR, visible, and SFG beams. Therefore, the resonance should be maximum if the S−C axis is tilted about 55° from the surface normal. These facts are clearly illustrated in Figure 3 for the calculated SFG signature for different values of θ. The comparison of the experimental and predicted ratios of the latter two SFG features indicates that the S−C axis is tilted from the surface normal, with the best fit for $\theta = 37°$.

Because the D mode has its infrared dipole moment perpendicular to the S−C axis (Figure 2), its sensitivity depends on both values of θ and ξ. For example, it is strongest when the TP ring rests flat on the surface. The B mode observation depends on both angles as well since this vibration dipole has a component perpendicular to the molecular axis. The SFG features induced by these modes near 720 and 980 cm^{-1} can be extinguished, as observed experimentally, if θ is close to 37° and $\xi = 0°$. The above orientations ($\theta = 37° \pm 10°$ and $\xi = 0° \pm 20°$) are to be compared with the value of $\theta = 24° \pm 5°$ determined in the latest angle-resolved XPS of TP adsorbed on Ag(111).[13] The error margins are estimated from the angular dependence of the theoretical spectra, with respect to the experimental data. The present SFG investigation is thus in line with those previous studies demonstrating that TP forms an ordered layer on Ag(111) leading to a S−C bond less inclined than that observed for an Au(111) substrate, where θ∼49°. Moreover, ξ close to 0° agrees with the general experimental observation[12] as well as the theoretical prediction[30] that aromatic chromophores predominantly adopt a herringbone packing.

Figure 1 also presents the SFG spectrum of NTT SAMs, which has not been obtained before in the 10−20 μm region. Studies of NTT SAMs on metals are scarce.[31,32] Because of the tendency of the thiolate group to adopt a SP hybridization when adsorbed on Ag[33] and/or in the presence of stronger interaction between end-groups,[10] thermal desorption spectroscopic data of NTT on Ag(111)[32] were interpreted assuming a linear Ag−S−C bond and a closed packed NTT film ordered in a herringbone configuration. Confirmation of that hypothesis based on the comparison between ab initio calculated SFG spectra and the present data is in progress and will be presented in a forthcoming paper.

Summary

In conclusion, SFG spectra of thiophenol (TP) and 2-naphthalenethiol monolayers confirm that films of these materials are ordered on Ag(111) surfaces. Ab initio theoretical SFG spectra show that the TP orientation can be determined from the relative intensities of the SFG resonances associated to the ring skeleton deformations in the spectral range 500−1050 cm^{-1}. We found that the S−C bond of TP is tilted from the surface normal and that the aromatic ring plane is perpendicular to the surface. A more accurate analysis will require the ab initio calculation of the TP properties taking account of the molecule chemisorption on the Ag surface.

Acknowledgment. We thank Dr. G. -Q. Lu for assistance during the SFG experiment. A.P., B.C., and Y.C. are Research Associate (R.A.), Senior R.A., and Postdoctoral Researcher, respectively, of the Belgian National Fund for Scientific Research (FNRS). This work was supported by the Belgian Fund for Joint Basic Research, by the Belgian Interuniversity Program on Quantum Size Effects in Nanostructured Materials PAI/IUAP 5/1 initiated by the Belgian Office for Scientific, Technical, and Cultural Affairs, and by the U.S. Department of Energy, Division of Materials Sciences under Award No. DEFG02-91ER45439, through the Frederick Seitz Materials Research Laboratory at the University of Illinois at Urbana-Champaign.

References and Notes

(1) Heeger, A. J. *Rev. Mod. Phys.* **2001**, *73*, 681−700.

(2) MacDiarmid, A. G. *Rev. Mod. Phys.* **2001**, *73*, 701−712.

(3) Marder, S. R.; Kippelen, B.; Jen, A. K. Y.; Peyghambarian, N. *Nature* **1997**, *388*, 845−851.

(4) Metzger, R. M.; Chen, B.; Höpfner, U.; Lakshmikantham, M. V.; Vuillaume, D.; Kawai, T.; Wu, X.; Tachinaba, H.; Hughes, T. V.; Sakurai, H.; Baldwin, J. W.; Hosch, C.; Cava, M. P.; Brehmer, L.; Ashwell, G. *J. Am. Chem. Soc.* **1997**, *119*, 10455−10466.

(5) Reed, M. A.; Zhou, C.; Muller, C. J.; Burgin, T. P.; Tour, J. *Science* **1997**, *278*, 252−254.

(6) Johansson, A.; Stafström, S. *Chem. Phys. Lett.* **2000**, *322*, 301−306.

(7) Wan, L.-J.; Terashima, M.; Noda, H.; Osawa, M. *J. Phys. Chem. B* **2000**, *104*, 3563−3569.

(8) Whelan, C. M.; Barnes, C. J.; Walker, C. G. H.; Brown, N. M. D. *Surf. Sci.* **1999**, *425*, 195−211.

(9) Whelan, C. M.; Smyth, M. R.; Barnes, C. J. *Langmuir* **1999**, *15*, 116−126.

(10) Tao, Y.-T.; Wu, C.-C.; Eu, J.-Y.; Lin, W.-L.; Wu, K.-C.; Chen, C.-H. *Langmuir* **1997**, *13*, 4018−4023.

(11) Sabatani, E.; Cohen-Boulakia, J.; Bruening, M.; Rubinstein, I. *Langmuir* **1993**, *9*, 2974−2981.

(12) Dhirani, A.-A.; Zehner, R. W.; Hsung, R. P.; Guyot-Sionnest, P.; Sita, L. R. *J. Am. Chem. Soc.* **1996**, *118*, 3319−3320.

(13) Frey, S.; Stadleer, V.; Heister, K.; Eck, W.; Zharnikov, M.; Grunze, M.; Zeysing, B.; Terfort, A. *Langmuir* **2001**, *17*, 2408−2415.

(14) Shen, W.; Nyberg, G. L.; Liesegang, J. *Surf. Sci.* **1993**, *298*, 143−160.

(15) Yeganeh, M. S.; Dougal, S. M.; Polizzotti, R. S.; Rabinowitz, P. *Phys. Rev. Lett.* **1995**, *74*, 1811−1814.

(16) Wei, X.; Zhuang, X.; Hong, S.-C.; Goto, T.; Shen, Y. R. *Phys. Rev. Lett.* **1999**, *82*, 4256−4259.

(17) Tadjeddine, A.; Guyot-Sionnest, P. *Electrochim. Acta* **1991**, *36*, 1849−1854.

(18) Peremans, A.; Caudano, Y.; Thiry, P.; Dumas, P.; Zheng, W.; Le Rille, A.; Tadjeddine, A. *Phys. Rev. Lett.* **1997**, *78*, 2999−3002.

(19) Mani, A. A.; Hollander, P.; Thiry, P. A.; Peremans, A. *Appl. Phys. Lett.* **1999**, *75*, 3066−3068.

(20) Mani, A. A.; Dreesen, L.; Hollander, P.; Humbert, C.; Caudano, Y.; Thiry, P. A.; Peremans, A. *Appl. Phys. Lett.* **2001**, *79*, 1945−1947.

(21) Mani, A. A.; Schultz, Z. D.; Gewirth, A. A.; White, J. O.; Caudano, Y.; Humbert, C.; Dreesen, L.; Thiry, P. A.; Peremans, A. *Opt. Lett.* **2004**, *29*, 274−276.

(22) Braun, R.; Casson, B. D.; Bain, C. D.; van der Ham, E. W. M.; Vrehen, Q. H. F.; Eliel, E. R.; Briggs, A. M.; Davies, P. B. *J. Chem. Phys.* **1999**, *110*, 4634−4640.

(23) Guyot-Sionnest, P. Nonlinear optical probes of surface dynamics: application to the vibrational dynamics of Si−H for Si(111)/H. In *Laser techniques for state-selected and state-to-state chemistry*; Cheuk-Yu, N., Ed.; Proc. SPIE: Bellingham, WA, 1993; Vol. 1858.

(24) Becke, A. D. *J. Chem. Phys.* **1993**, *98*, 5648−5652.

(25) Frisch, M. J.; Trucks, G. W.; Schlegel, H. B.; Scuseria, G. E.; Robb, M. A.; Cheeseman, J. R.; Zakrzewski, V. G.; Montgomery, J. A., Jr.; Stratmann, R. E.; Burant, J. C.; Dapprich, S.; Millam, J. M.; Daniels, A. D.; Kudin, K. N.; Strain, M. C.; Farkas, O.; Tomasi, J.; Barone, V.; Cossi, M.; Cammi, R.; Mennucci, B.; Pomelli, C.; Adamo, C.; Clifford, S.; Ochterski, J.; Petersson, G. A.; Ayala, P. Y.; Cui, Q.; Morokuma, K.; Malick, D. K.; Rabuck, A. D.; Raghavachari, K.; Foresman, J. B.; Cioslowski, J.; Ortiz, J. V.; Stefanov, B. B.; Liu, G.; Liashenko, A.; Piskorz, P.; Komaromi, I.; Gomperts, R.; Martin, R. L.; Fox, D. J.; Keith, T.; Al-Laham, M. A.; Peng, C. Y.; Nanayakkara, A.; Gonzalez, C.; Challacombe, M.; Gill, P. M. W.; Johnson, B. G.; Chen, W.; Wong, M. W.; Andres, J. L.; Head-Gordon, M.; Replogle, E. S.; Pople, J. A. *Gaussian 98*, revision A.1; Gaussian, Inc.: Pittsburgh, PA, 1998.

(26) Komornicki, A.; Fitzgerald, G. J. *J. Chem. Phys.* **1993**, *98*, 1398−1421 and references therein.

(27) Scott, A. P.; Radom, L. *J. Chem. Phys.* **1996**, *100*, 16502−16513.

(28) Champagne, B. *Chem. Phys. Lett.* **1996**, *57*, 261−265.

(29) Humbert, C.; Buck, M.; Calderone, A.; Vigneron, J.-P.; Meunier, V.; Champagne, B.; Zheng, W.-Q.; Tadjeddine, A.; Thiry, P. A.; Peremans, A. *Phys. Status Solidi A* **1999**, *175*, 129−136.

(30) Chang, S.-C.; Chao, I.; Tao, Y.-T. *J. Am. Chem. Soc.* **1994**, *116*, 6792−6805.

(31) Kolega, R. R.; Schlenoff, J. B. *Langmuir* **1998**, *14*, 5469−5478.

(32) Kim, C.; Sim, J. H.; Yan, X. M.; White, J.-M. *Langmuir* **2002**, *18*, 3159−3166.

(33) Zharnikov, M.; Frey, E.; Rong, H.; Yang, Y.-J.; Heister, K.; Buck, M.; Grunze, M. *Phys. Chem. Chem. Phys.* **2000**, *2*, 3359−3362.